

Provided for non-commercial research and education use.  
Not for reproduction, distribution or commercial use.



This article appeared in a journal published by Elsevier. The attached copy is furnished to the author for internal non-commercial research and education use, including for instruction at the authors institution and sharing with colleagues.

Other uses, including reproduction and distribution, or selling or licensing copies, or posting to personal, institutional or third party websites are prohibited.

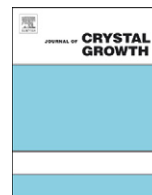
In most cases authors are permitted to post their version of the article (e.g. in Word or Tex form) to their personal website or institutional repository. Authors requiring further information regarding Elsevier's archiving and manuscript policies are encouraged to visit:

<http://www.elsevier.com/copyright>



Contents lists available at ScienceDirect

Journal of Crystal Growth

journal homepage: [www.elsevier.com/locate/jcrysgro](http://www.elsevier.com/locate/jcrysgro)

## Epitaxial growth of GdN on silicon substrate using an AlN buffer layer

F. Natali<sup>a,\*</sup>, N.O.V. Plank<sup>a</sup>, J. Galipaud<sup>a</sup>, B.J. Ruck<sup>a</sup>, H.J. Trodahl<sup>a</sup>, F. Semond<sup>b</sup>, S. Sorieul<sup>c</sup>, L. Hirsch<sup>d</sup>

<sup>a</sup> MacDiarmid Institute for Advanced Materials and Nanotechnology, School of Chemical and Physical Sciences, Victoria University of Wellington, PO Box 600, Wellington 6140, New Zealand

<sup>b</sup> Centre de Recherche sur l'Hetero-Epitaxie et ses Applications, Centre National de la Recherche Scientifique, Rue Bernard Gregory, 06560 Valbonne, France

<sup>c</sup> Centre d'Etudes Nucléaires de Bordeaux-Gradignan IN2P3, UMR 5797, Université de Bordeaux 1, Chemin du solarium BP120, 33175 Gradignan Cedex, France

<sup>d</sup> Université Bordeaux 1, Laboratoire d'Intégration du Matériau au Système – CNRS UMR 5218, ENSCPB, 16, Avenue Pey Berland, 33607 Pessac Cedex, France

### ARTICLE INFO

#### Article history:

Received 25 June 2010

Received in revised form

19 August 2010

Accepted 10 September 2010

Communicated by K.H. Ploog

Available online 17 September 2010

#### Keywords:

A3. Molecular beam epitaxy

B1. Nitrides

B2. Magnetic materials

B2. Semiconducting materials

### ABSTRACT

We report on the epitaxial growth of the intrinsic ferromagnetic semiconductor GdN on Si (1 1 1) substrates buffered by a thick AlN layer, forming a heteroepitaxial system with promise for spintronics. Growth is achieved by depositing Gd in the presence of unactivated N<sub>2</sub> gas, demonstrating a reactivity at the surface that is sufficient to grow near stoichiometric GdN only when the N<sub>2</sub>:Gd flux ratio is at least 100. Reflection high-energy electron diffraction and X-ray diffraction show fully (1 1 1)-oriented epitaxial GdN films. The epitaxial quality of the films is assessed by Rutherford backscattering spectroscopy carried out in random and channelling conditions. Magnetic measurements exhibit a Curie temperature at 65 K and saturation magnetisation of 7 μ<sub>B</sub>/Gd in agreement with previous bulk and thin-film data. Hall effect and resistance data establish that the films are heavily doped semiconductors, suggesting that up to 1% of the N sites are vacant.

© 2010 Elsevier B.V. All rights reserved.

### 1. Introduction

A major challenge for the next generation of spintronic devices is the implementation of ferromagnetic semiconductor thin films as spin injectors and detectors [1,2]. Spin-polarised carrier injection cannot be accomplished efficiently from metals [3] and coupled with the rarity of intrinsic ferromagnetic semiconductors this has driven intensive study of diluted magnetic semiconductors [4]. Chief among these is the doped III–V compound (Ga,Mn)As. These materials suffer from a number of drawbacks; they (i) require magnetic-ion doping well above the solubility limit and (ii) must be hole doped to above the degenerate limit, preventing independent control of the carrier concentration and charge sign. That problem is further exacerbated by carrier doping that results from the transition metal ions themselves.

Rare-earth nitrides (RN) were studied already 50 years ago, but only recently have been grown with sufficient stoichiometry to establish their properties confidently. Across the rare-earth series they display a wide range of transport and magnetic properties, though most are ferromagnetic semiconductors at low temperature. GdN is the most thoroughly studied, in part because of the maximum spin moment of 7 μ<sub>B</sub> and zero orbital angular momentum in the half-filled 4f shell of Gd<sup>3+</sup>. Historically its conducting nature was uncertain, due to doping by a high

concentration of N vacancies [5–8]. GdN films with low vacancy densities have resistivities of moderately doped semiconductors. Its optical band gap is 0.9 eV in the ferromagnetic phase and the band structure tuned to this gap shows a semiconductor with an indirect gap of 0.43 eV [9]. That band structure has been confirmed by resonant and non-resonant X-ray spectroscopy [10]. The spin splitting is about 0.4 eV (4500 K) in both band edges, with the majority spin (parallel to the Gd 4f shell spin) having lower energy in the conduction band and higher energy in the valence band. Thus carriers at both edges, electrons and holes, are in majority-spin bands. Any GdN-based device (diode, transistor) that requires doping or accumulating carriers into the band edges will involve transport of carriers with only that majority spin state. Eu, with its propensity to form the divalent state with a half-filled 4f shell, has a metastable monoxide, EuO, which shows magnetic properties similar to GdN. However the band structures of the two compounds differ strongly, with the 4f character of the EuO valence band that is too flat to form usefully mobile holes [11–13].

GdN adopts a face centred cubic (NaCl) structure with a lattice parameter of 0.498 nm. (1 0 0)-oriented epitaxial films have been grown on both YSZ(1 0 0) [14] and MgO(1 0 0) [15], and the propensity of GdN to be strongly textured in the (1 1 1) direction [7] encouraged Scarpulla et al. [16] to grow onto the GaN(0 0 0 1) surface, a technologically important material for the fabrication of opto-electronic devices and high power transistors. Silicon, on the other hand, is attractive as an alternative to these substrates because of its low cost, large scale availability and high thermal

\* Corresponding author.

E-mail address: [franck.natali@vuw.ac.nz](mailto:franck.natali@vuw.ac.nz) (F. Natali).

and electrical conducting properties. In addition, silicon remains the most well-developed and heavily exploited semiconductor, so any future exploitation will place a premium on integration with Si. A similar premium was placed on epitaxial III–V/Si integration, which has recently led to the monolithic integration of GaN-based transistors and silicon MOSFETs on a silicon substrate [17].

The 7.5% lattice mismatch between GdN and Si, though relatively severe, is not an insurmountable problem; more problematic is the reactivity of Gd with Si, encouraging the formation of a metallic  $\text{GdSi}_x$  layer with a surface of poor quality and preventing the growth of high quality GdN layers [18]. In this paper, we show that this reaction is avoided by using a wurtzite (0 0 0 1) AlN buffer layer on top of the silicon (1 1 1) substrate. The structural, magnetic and transport properties of the epitaxial (1 1 1)-oriented GdN thin films ( $\leq 25$  nm) grown on this AlN buffer layer were investigated through combined measurements of reflection high-energy electron diffraction (RHEED), X-ray diffraction (XRD), Rutherford backscattering spectroscopy (RBS), Hall effect, temperature-dependent magnetisation and resistivity.

## 2. Experimental

The films in this study consist of GdN grown on a 100 nm (0 0 0 1) wurtzite AlN buffer layer capped with 35 nm of polycrystalline AlN. The AlN(0 0 0 1) buffer layer, which successfully prevents silicide formation, was grown ex situ on Si(1 1 1) substrates by using the molecular beam epitaxy method in the RIBER Compact 21 system. Standard effusion cell is used for Al while nitrogen species are provided by using ammonia. Details of the growth procedure and the properties of the epitaxial AlN buffer layer can be found in Refs. [19,20]. These templates were then placed in a UHV chamber pumped to a base pressure of  $\sim 8 \times 10^{-9}$  Torr and outgassed at 600 °C for 1 h to remove any possibly adsorbed contaminants and produce a clean surface. The surface was monitored by RHEED and a disappearing filament pyrometer was employed to measure the growth temperature. The Gd flux and GdN growth were at a rate of 60–80 nm/h, under a pressure of pure  $\text{N}_2$  ranging from  $4 \times 10^{-5}$  to  $4 \times 10^{-4}$  Torr with the substrates held at temperatures of 650–750 °C. Under these conditions the  $\text{N}_2$  flux on the growth surface is  $10^2$ – $10^3$  times larger than the Gd flux; for substantially lower  $\text{N}_2$  pressure the films were severely Gd rich. The polycrystalline AlN capping layer was grown at 300 K by evaporating Al in the presence of activated nitrogen.

The thicknesses of the layers were determined by RBS experiments using 2 MeV  $^4\text{He}^+$  ion beams with 160° scattering angle. The epitaxial quality of the films is assessed by Rutherford backscattering spectroscopy carried out in random and channelling conditions. The random spectrum was done with a rotating sample with 5° tilt angle. The crystalline structure has also been assessed by XRD  $2\theta$ – $\theta$  scans. The temperature and field-dependence of magnetisation were measured with a superconducting quantum interference device for an in-plane field orientation. Electron transport measurements have been carried out using a van der Pauw configuration.

## 3. Results and discussion

Fig. 1 displays the variation of the in-plane surface lattice parameter during growth. The onset of plastic relaxation by misfit dislocation generation appears only after  $\sim 2.5$  monolayers (MLs), i.e., about 4.5 Å, as expected in view of the large lattice mismatch between AlN and GdN ( $\sim +13\%$ ). A two dimensional growth mode is observed, even after the onset of plastic relaxation (see inset Fig. 1). Further growth allows a rapid relaxation of the GdN lattice

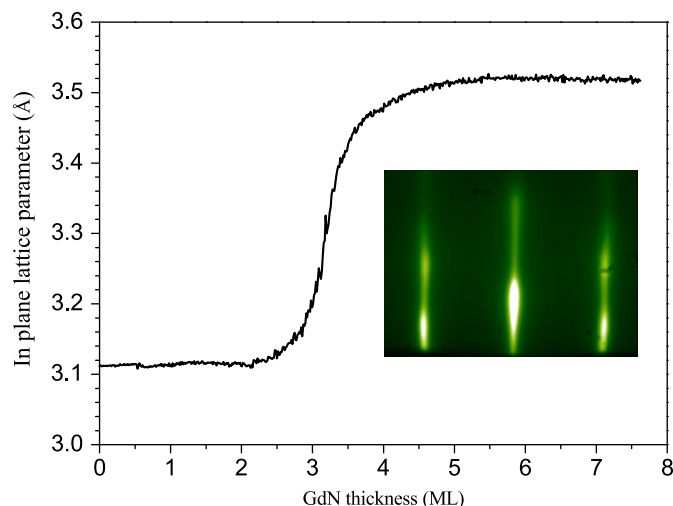


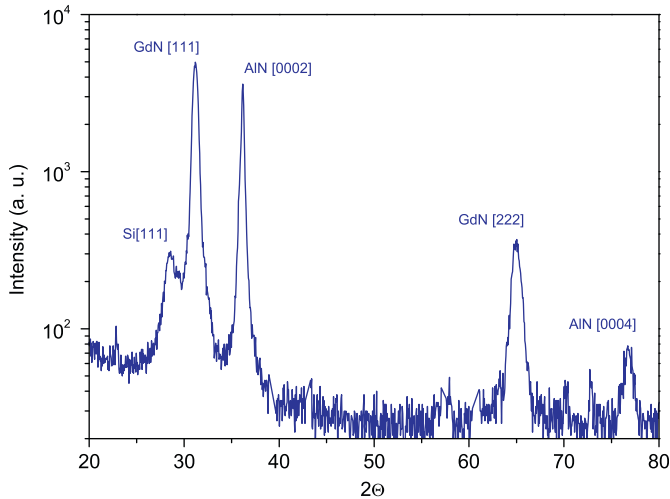
Fig. 1. Variation of in-plane surface lattice parameter during the growth of GdN on AlN as measured by RHEED. The inset shows the RHEED pattern along the Si [1 1 0] azimuth of a 14 nm thick GdN layer.

as a fully relaxed GdN layer is obtained after only 6 MLs. The in-plane lattice parameter deduced from the RHEED pattern along the Si [1 1 0] azimuth is 3.52 Å, in agreement with the bulk GdN value ( $a_{\text{GdN}(111)} = a_{\text{GdN}}/\sqrt{2} = 3.521$  Å). By increase in the thickness a change in the RHEED pattern occurs after  $\sim 25$  nm as it becomes spottier, with double spots indicating the formation of twinning. Subsequent growth of GdN on such twinned films leads to the formation of circle-like features that appear as reported during the growth of (0 0 1) oriented GdN on MgO [15].

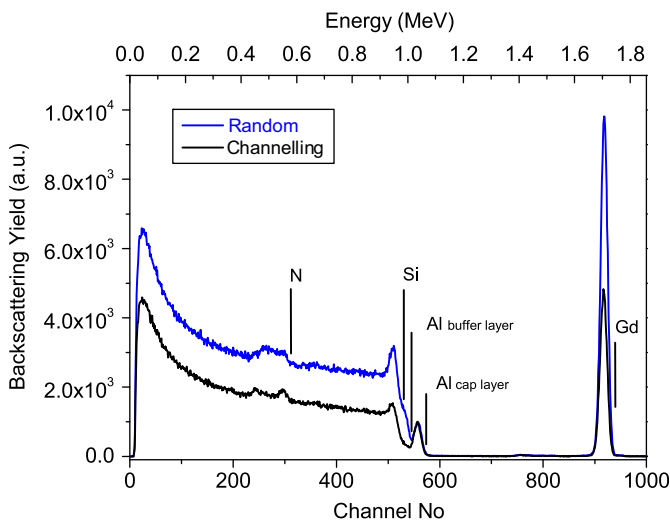
Evidently the reaction of Gd with  $\text{N}_2$  takes place at the surface to form an epitaxial GdN layer, even in the absence of activated  $\text{N}_2$ . Such growth has previously been demonstrated for polycrystalline films of GdN, SmN, DyN, ErN and LuN [5,21], but this is its first demonstration for epitaxial-film growth. It is worth noting that all previous epitaxial growths have used activated nitrogen or  $\text{NH}_3$  as nitrogen precursor [14–16], in particular for the growth of (1 1 1)-oriented GdN on GaN substrates [16].

Fig. 2 displays the XRD  $2\theta$ -scan of a 14 nm thick GdN film confirming the epitaxial character. In addition to the peaks of AlN and Si we observe only the (1 1 1) and (2 2 2) reflections of GdN. Clearly the hexagonal face of AlN favours a fully (1 1 1)-oriented GdN film. Using the Scherrer formula, we extract a coherence length of  $\sim 15$  nm, somewhat smaller than the  $\sim 26$  nm for GdN grown on nearly lattice-matched YSZ [14]. This is not unforeseen for the 13% lattice mismatch between AlN and GdN and the high threading dislocation density in the AlN buffer layer,  $5 \times 10^{11} \text{ cm}^{-2}$  [20].

Due to decomposition in air of the REN film, high resolution cross-section microscopy in order to determine the epitaxial quality of the films is impossible. To obtain more qualitative information on the epitaxial nature of the GdN layer we performed RBS measurement in random and channelling conditions. Fig. 3 shows the random (blue) and aligned (black) RBS spectra of a 20.5 nm thick GdN layer. The reduction in yield associated with channelling is clear evidence of the epitaxial nature of the GdN layer; note that the reduction of the Gd signal is by a very similar fraction to that found from both the Si substrate and the AlN buffer layer, while as expected there is no evidence of channelling in the polycrystalline AlN cap layer. However, while no accurate  $\chi_{\text{min}}$  value can be determined due to the thinness of the GdN layer, the strong yield reduction is a proof of the low lattice disorder in the film. Finally, although the nitrogen RBS signal overlaps with that of silicon, the resolution is sufficient to give the Gd:N ratio of  $1.0 \pm 5\%$  from the random spectra.



**Fig. 2.** X-ray diffraction scan of an AlN-capped 14 nm thick GdN film grown on an AlN/Si(1 1 1) sequence under  $4 \times 10^{-5}$  Torr of  $N_2$ . This typical  $\theta$ - $2\theta$ -scan XRD scan shows that in addition to the peaks of AlN and Si only the (1 1 1) and (2 2 2) reflections of GdN are present in these films. These data demonstrate the wurtzite (0 0 0 1) surface of the AlN buffer layer favours the growth of fully (1 1 1)-oriented GdN film.



**Fig. 3.** Rutherford backscattering spectroscopy measurements in random (blue) and channelling (black) conditions of AlN/20.5 nm GdN/AlN/Si(1 1 1) sequence. The lines (labelled Gd, Al, Si and N) indicate the onset of backscattering energy for these elements at the surface. (For interpretation of the references to colour in this figure legend, the reader is referred to the web version of this article.)

We have found no evidence of crystalline-quality or composition dependence on either the substrate temperature (650–750 °C) or the  $N_2$  pressure across the ranges explored, though as will be discussed below there is indirect evidence of improved stoichiometry in films grown at higher  $N_2$  pressure. Not surprisingly, films grown at the much lower temperature,  $< 100$  °C, are polycrystalline. It is interesting to distinguish the temperature range with the few existing reports of the epitaxial growth using activated nitrogen. Epitaxial GdN films grown by PLD showed no systematic variation in quality across the temperature range 700–850 °C [14]. On the other hand, Scarpulla et al. [16] reported that deposition at temperatures higher than 450 °C did not yield GdN films on GaN substrates.

Fig. 4 shows the temperature- and field-dependence of magnetisation for an in-plane field orientation; a Curie temperature of  $T_c \approx 65$  K is deduced from both the onset of hysteretic magnetisation and by the temperature dependence of the inverse susceptibility in

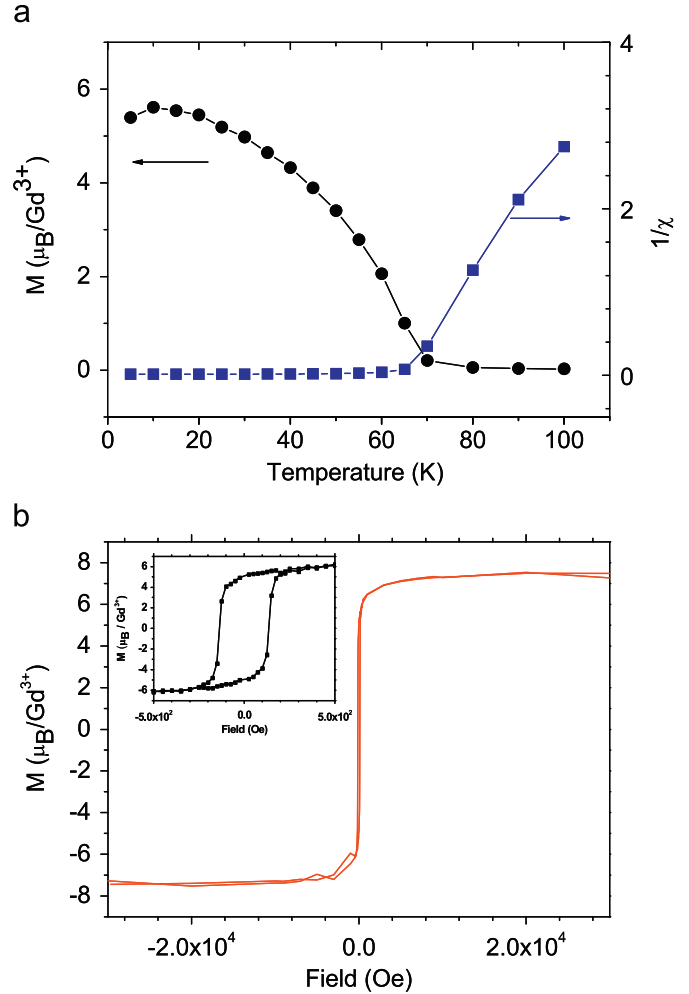


**Fig. 4.** Temperature-dependent magnetisation and inverse susceptibility in an applied field of 25 mT (a) and field-dependent of the magnetisation at a temperature of 10 K (b) of a 14 nm thick GdN layer. The inset is a magnification of the magnetisation at low field showing a coercive field of about 125 Oe.

the paramagnetic phase (Fig. 4a). The magnetic hysteresis at 10 K shows a coercive field of 125 Oe and a saturation magnetisation  $M_{sat}$  of  $7.5 \pm 0.5 \mu_B/Gd^{3+}$ , in agreement with the expected  $7.0 \mu_B/Gd^{3+}$  for a half-filled  $4f$  shell (Fig. 4b). The coercive field is a factor of about two smaller than we have reported in films with a similar crystallite size grown on YSZ, suggesting that even smaller coercive fields may be typical of well-ordered GdN [14]. Note that oxygen contamination as small as a few percent is reported to increase the coercive field to thousands of Oe and to decrease the Curie temperature of GdN [22]. The very small coercive field we measure supports the absence of significant oxygen that has also been noted in RBS data, establishing the efficacy of the AlN cap as a passivation layer.

The Hall effect in these films (Fig. 5) shows n-type conduction, enhanced by an extraordinary Hall effect in the ferromagnetic state. Note that this 14 nm thick film was grown at the minimum  $N_2$  pressure,  $4 \times 10^{-5}$  Torr. The carrier concentration inferred from the high-field slopes in Fig. 5 is  $2.4 \times 10^{21} \text{ cm}^{-3}$  at ambient temperature, falling to  $0.77 \times 10^{21} \text{ cm}^{-3}$  at 90 K before rising to  $1 \times 10^{21} \text{ cm}^{-3}$  in the ferromagnetic state. Such a rise in the ferromagnetic state is exactly as expected in view of the reduced band gap below the Curie temperature. However below 50 K the carrier concentration again falls, signalling a ferromagnetic semiconductor ground state. The heavy doping is dominated by nitrogen vacancies, and assuming that each nitrogen vacancy provides three electrons this suggests a vacancy density of the order 1%.

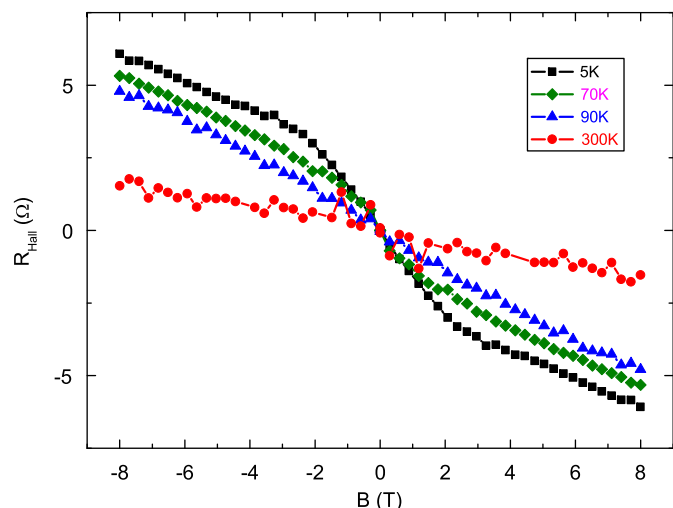


Fig. 5. Hall resistance for the 14 nm thick GdN films grown under  $4 \times 10^{-5}$  Torr of  $N_2$  as a function of applied field at different temperatures 300, 90, 70 and 5 K showing the transition between paramagnetic and ferromagnetic phases.

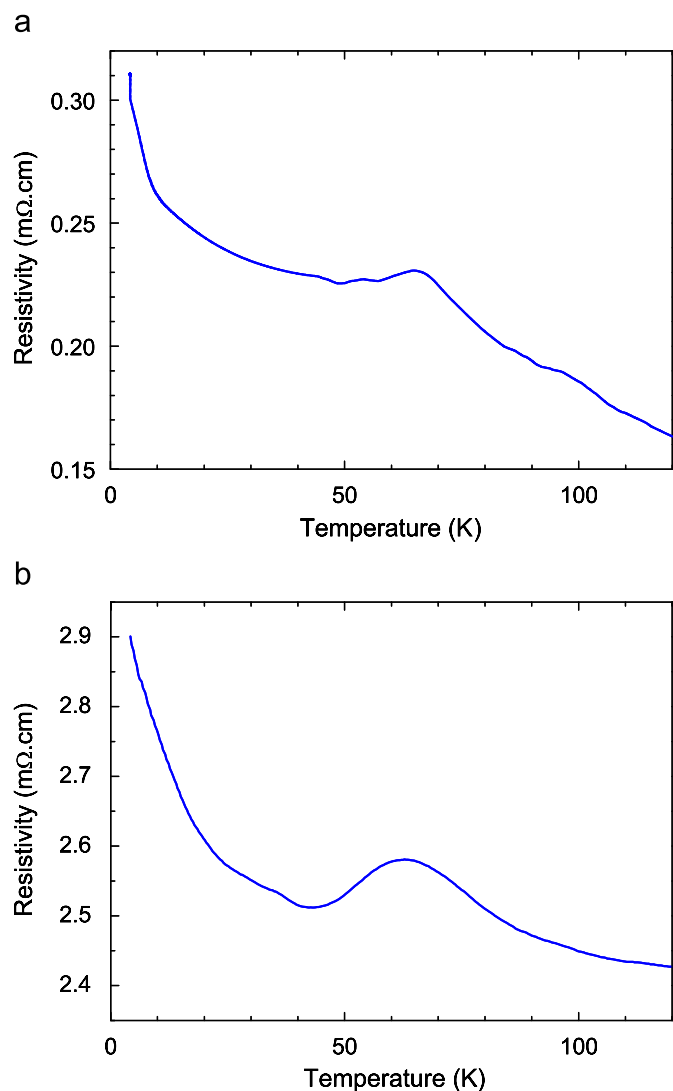


Fig. 6. Temperature-dependent resistivity of a 14 nm thick GdN film grown under (a)  $4 \times 10^{-5}$  Torr of  $N_2$  and (b)  $4 \times 10^{-4}$  Torr  $N_2$  with a peak at the Curie temperature.

The temperature-dependent resistivity of the same film, seen in Fig. 6a, shows the previously reported anomaly as the gap narrows across the Curie temperature [7,8,14,16,25] and a diverging semiconductor-like resistivity below 10 K. Our data differ in this respect from those reported by Scarpulla et al. [16] for (1 1 1)-oriented GdN epitaxial films grown on GaN since they observed a metallic conductivity for temperature down to 10 K. The ambient-temperature resistivity of  $0.1 \text{ m}\Omega \text{ cm}$  gives a mobility of  $\sim 15 \text{ cm}^2/\text{V s}$ , similar to previous data on a PLD-grown epitaxial GdN layer on YSZ [14] and plasma-assisted MBE grown epitaxial GdN layer on GaN [16]. From these values and assuming a free electron effective mass  $m^*/m=1$ , we calculate a mean free path of 11 nm, comparable to the layer thickness and the crystallite radius (15 nm) inferred from XRD spectra.

Fig. 6b shows the resistivity of film grown at a  $N_2$  pressure of  $4 \times 10^{-4}$  Torr. The resistivity is a factor of ten larger, signalling a reduced concentration of N vacancies in this film grown with a larger  $N_2$  pressure, as has been seen previously in polycrystalline films [7]. However, the anomaly and low-temperature rise show remarkable similarity to those in Fig. 6a.

The thickness of AlN buffer in this study, required to avoid a short circuit through the Si substrate, has so far prevented a study of direct injection into the Si. We anticipate that successful epitaxy can be performed on thinner AlN, as reported for the realisation of group III-nitrides-based devices [17,19]. It is of interest to note that the AlN buffer layer not only prevents the problematic silicide formation but can also act as template for the integration of GdN into group III-nitrides, a technologically important family for the fabrication of opto-electronic devices and high power transistors [31].

#### 4. Conclusion

Summarising the experiments, we have grown epitaxial films of the ferromagnetic semiconductor GdN on Si(1 1 1), preventing the problematic silicide formation by the use of an AlN buffer layer. We showed that GdN thin films can be grown epitaxially using inert nitrogen gas rather than using a  $N_2$  plasma source or ammonia as nitrogen precursor. The films have a Curie temperature of 65 K and a saturation magnetisation in agreement with previous data on GdN. Electrical measurements showed that the films are heavily doped by N vacancies. The demonstration of the growth of GdN films on buffered silicon paves the way for the future integration of this intrinsic ferromagnetic semiconductor on silicon that has potential roles in spintronics.

#### Acknowledgements

The authors are grateful to J. Stephen, A Hyndman, G. Williams and P. Murmu for technological help for SQUID and Hall Effect measurements. This research was supported by the New Economy Research Fund (Contract VICX0808) and the Marsden Fund (08-VUW-030).

#### References

- [1] S. von Molnár, D. Reed, Proc. IEEE 91 (2003) 715.
- [2] S.W. Wolf, D.D. Awschalom, R.A. Buhrman, J.M. Daughton, S. von Molnár, M.L. Roukes, A.Y. Chtchelkanova, D.M. Treger, Science 294 (2001) 1488.
- [3] G. Schmidt, D. Ferrand, L.W. Molenkamp, A.T. Filip, B.J. vanWees, Phys. Rev. B 62 (2000) R4790.
- [4] T. Dietl, H. Ohno, F. Matsukura, J. Cibert, D. Ferrand, Science 287 (2000) 1019.
- [5] J.Q. Xiao, C.L. Chien, Phys. Rev. Lett. 76 (1996) 1727.
- [6] P. Wachter, E. Kaldis, Solid State Commun. 34 (1980) 241.

- [7] S. Granville, B.J. Ruck, F. Budde, A. Koo, D.J. Pringle, F. Kuchler, A.R.H. Preston, D.H. Housden, N. Lund, A. Bittar, G.V.M. Williams, H.J. Trodahl, *Phys. Rev. B* 73 (2006) 235335.
- [8] F. Leuenberger, E. Parge, W. Felsch, K. Fauth, M. Hessler, *Phys. Rev. B* 72 (2005) 014427.
- [9] H.J. Trodahl, A.R.H. Preston, J. Zhong, B.J. Ruck, N.M. Strickland, C. Mitra, W.R.L. Lambrecht, *Phys. Rev. B* 76 (2007) 085211.
- [10] A.R.H. Preston, B.J. Ruck, W.R.L. Lambrecht, L.F.J. Piper, J.E. Downes, K.E. Smith, H.J. Trodahl, *Appl. Phys. Lett.* 96 (2010) 032101.
- [11] A. Schmehl, V. Vaithyanathan, A. Herrnberger, S. Thiel, C. Richter, M. Liberati, T. Heeg, M. Röckerath, L. Fitting Kourkoutis, S. Mühlbauer, P. Böni, D.A. Müller, Y. Barash, J. Schubert, Y. Idzerda, J. Mannhart, D.G. Schlom, *Nat. Mater.* 6 (2007) 882.
- [12] D.B. Gosh, M. De, S.K. De, *Phys. Rev. B* 70 (2004) 115211.
- [13] N. Schiller, W. Nolting, *Solid State Commun.* 118 (2001) 173.
- [14] B.M. Ludbrook, I.L. Farrell, M. Kuebel, B.J. Ruck, A.R.H. Preston, H.J. Trodahl, L. Ranno, R.J. Reeves, S.M. Durbin, *J. Appl. Phys.* 106 (2009) 063910.
- [15] J.W. Gerlach, J. Mennig, B. Rauschenbach, *Appl. Phys. Lett.* 90 (2007) 061919.
- [16] M.A. Scarpulla, C.S. Gallinat, S. Mack, J.S. Speck, A.C. Gossard, *J. Cryst. Growth* 311 (2009) 1239.
- [17] P.N. Chyurlia, F. Semond, T. Lester, J.A. Bardwell, S. Rolfe, H. Tang, N.G. Tarr, *Electron. Lett.* 46 (2010) 240.
- [18] C.-J. Youn, K. Jungling, W.W. Grannemann, *J. Vac. Sci. Technol. A* 6 (1988) 2474.
- [19] F. Semond, Y. Cordier, N. Grandjean, F. Natali, B. Damianno, S. Vézian, J. Massies, *Phys. Status Solidi A* 188 (2001) 501.
- [20] F. Natali, F. Semond, J. Massies, D. Byrne, S. Lügt, O. Tottereau, P. Vennéguès, E. Dogheche, E. Dumont, *Appl. Phys. Lett.* 82 (2003) 1386.
- [21] S. Granville, C. Meyer, A.R.H. Preston, B.M. Ludbrook, B.J. Ruck, H.J. Trodahl, T.R. Paudel, W.R.L. Lambrecht, *Phys. Rev. B* 79 (2009) 054301.
- [22] K. Khazen, H.J. von Bardeleben, J.L. Cantin, A. Bittar, S. Granville, H.J. Trodahl, B.J. Ruck, *Phys. Rev. B* 74 (2006) 245330.
- [25] H.T. He, C.L. Yang, W.K. Ge, J.N. Wang, X. Dai, Y.Q. Wang, *Appl. Phys. Lett.* 87 (2005) 162506.
- [31] B. Gil, in: *Group III Nitride Semiconductor Compounds*, Oxford University Press, Oxford, 1998.